Spectroscopic Properties and Crystal Structures of Luminescent Linear Tri- and Tetra-nuclear Gold(I) Complexes with Bis(diphenylphosphinomethyl)phenylphosphine Ligand†

Dan Li,[a] Chi-Ming Che,[*,a] Shie-Ming Peng,[b] Shiuh-Tzung Liu,[b] Zhong-Yuan Zhou,[c] and Thomas C. W. Mak[c]

[a] Department of Chemistry, The University of Hong Kong, Pokfulam Road, Hong Kong

[b] Department of Chemistry, National Taiwan University, Taipei, Taiwan

[c] Department of Chemistry, The Chinese University of Hong Kong, Shatin, New Territories, Hong Kong

Reaction of $[AuCl_4]^-$ with 2,2′-thiodiethanol in methanol generated Au^I in situ, which reacted with bis(diphenylphosphinomethyl)phenylphosphine (dpmp) and NaSCN to give $[Au_4(dpmp)_2(SCN)_2]^{2+}$ and $[Au_3(dpmp)_2]^{3+}$. The crystal structures of $[Au_4(dpmp)_2(SCN)_2][SCN]Cl$ and $[Au_3(dpmp)_2][SCN]_3$ have been determined: $[Au_3(dpmp)_2][SCN]_3$, monoclinic, space group $P2_1/n$, $a = 12.474(4)$, $b = 25.575(4)$, $c = 20.182(6)$ Å, $\beta = 92.61(3)°$ and $Z = 4$; $[Au_4(dpmp)_2(SCN)_2][SCN]Cl$, space group $P\bar{1}$ (no. 2), $a = 13.799(2)$, $b = 14.061(2)$, $c = 19.390(4)$ Å, $\alpha = 88.46(2)$, $\beta = 75.41(1)$, $\gamma = 74.58(1)°$ and $Z = 2$. They comprise nearly linear Au_3 and Au_4 chains with Au–Au–Au angles of $167.21(2)°$ for $[Au_3(dpmp)_2][SCN]_3$, $160.0(1)$ and $167.2(1)$ for $[Au_4(dpmp)_2(SCN)_2][SCN]Cl$. A weak Au^I–Au^I bonding interaction is anticipated in view of the intramolecular $Au \cdots Au$ separations. Both complexes show room-temperature photoluminescence. The red shift in the $d_\sigma \rightarrow p_\sigma$ transition energy from $[Au_2(dppm)_2]^{2+}$ [dppm = bis(diphenylphosphino)methane] to $[Au_3(dpmp)_2]^{3+}$ and to $[Au_4(dpmp)_2(SCN)_2]^{2+}$ has been attributed to the bonding interactions between adjacent P_2Au units. The photophysical properties of $[Au_3(dpmp)_2][SCN]_3$ are discussed.

The novel photophysical and photochemical properties of polynuclear d^{10} metal complexes have received considerable attention in our laboratory.[1] Although the photophysical properties of luminescent dimeric gold(I) complexes have been studied extensively,[1a,2–4] related studies on corresponding tri- and tetra-meric complexes are sparse. The ligand bis(diphenyl-phosphinomethyl)phenylphosphine (dpmp) has previously been employed to construct luminescent trinuclear metal complexes such as $[Rh_3(dpmp)_2(MeCN)_6]^{2+}$ 1,[5] $[Ag_3(dpmp)_2$-$(MeCN)_2(ClO_4)]^+$ 2,[1c] and $[Cu_3(dpmp)_2(MeCN)_2(\mu\text{-}X)_2]^+$ 3 (X = Cl or I).[1e] Herein is described the synthesis, crystal structure and spectroscopic properties of a linear trimeric gold(I) complex $[Au_3(dpmp)_2][SCN]_3$. A tetrameric complex $[Au_4(dpmp)_2(SCN)_2][SCN]Cl$, which was obtained as a side product of the reaction, has also been characterized by X-ray crystallography.

Experimental

The salt $K[AuCl_4]$ (Johnson Matthey Chemicals) and 2,2′-thiodiethanol (Strem Chemicals) were used without further purification. The ligand dpmp was prepared by a published method.[6] The salt $[Au(PPh_3)_2][CF_3SO_3]$ was prepared by metathesis of $[Au(PPh_3)_2Cl]^7$ with $Ag[CF_3SO_3]$ in acetone followed by precipitation with diethyl ether. Acetonitrile (Ajax AR) was distilled over $KMnO_4$ and CaH_2 under nitrogen. Solvents for synthesis were of analytical quality used without further purification.

Synthesis of $[Au_3(dpmp)_2][SCN]_3$.—2,2′-Thiodiethanol (0.5 cm³) was added with stirring to a methanolic solution of

$K[AuCl_4]$ (0.2 g, 0.53 mmol in 10 cm³ methanol). Solid dpmp (0.18 g, 0.36 mmol) was added when the solution became clear and colourless. The solution was heated to 40–50 °C for 0.5 h, then NaSCN (0.05 g, 0.62 mmol) was added to give a clear yellow solution. Yellow crystals were obtained upon standing of the solution in air at room temperature for a few days. The product was recrystallized from hot methanol (Yield ≈ 60%) (Found: C, 44.80; H, 3.10; N, 2.30. Calc. for $C_{67}H_{58}Au_3N_3P_6S_3$: C, 45.25; H, 3.25; N, 2.35%); $\nu(SC\equiv N)$ 2051 cm⁻¹.

Physical Measurements and Instrumentation.—The UV–VIS spectra were recorded on a Milton Roy Spectronic 3000 diode-array spectrophotometer and steady-state emission spectra on a SPEX Fluorolog-2 spectrofluorometer. Lifetime measurements were performed with a Quanta Ray DCR-3 Nd-YAG laser (pulse output 355 nm, 8 ns). Solutions for photochemical experiments were degassed by at least four freeze–pump–thaw cycles.

X-Ray Crystallography.—$[Au_3(dpmp)_2][SCN]_3$. X-Ray diffraction data were collected on a Nonius CAD 4 diffracto-meter using the θ–2θ scan mode $[2\theta_{max} = 44.9°$, scan speed $(16.48/7)$–$(16.48/2)°$ min⁻¹] at National Taiwan University. The unit cell dimensions were obtained from 25 reflections in the range $20 < 2\theta < 30.5°$.

Crystal data. $M = 1778.12$ monoclinic, space group $P2_1/n$, $a = 12.474(4)$, $b = 25.575(4)$, $c = 20.182(6)$ Å, $\beta = 92.61(3)°$, $U = 6432(3)$ Å³, $\lambda = 0.710\,69$ Å, $Z = 4$, $D_c = 1.836$ g cm⁻³, crystal dimensions $0.20 \times 0.20 \times 0.20$ mm, $\mu(\text{Mo-K}\alpha) = 7.09$ mm⁻¹, $F(000) = 3423$.

The last least-squares cycle was calculated with 140 atoms, 740 parameters and 5716 ($|I_o| > 2\sigma|I_o|$) out of 8386 unique reflections; $R = 0.042$, $R' = 0.035$, $w = 1/\sigma^2(F_o)$. The final Fourier difference map showed residual extrema in the range 1.65 to -1.13 e Å⁻³.

$[Au_4(dpmp)_2(SCN)_2][SCN]Cl$. The complex was obtained as golden-yellow flat prisms.

Table 1 Atomic parameters of non-hydrogen atoms of $[Au_3(dpmp)_2][SCN]_3$

Atom	x	y	z	Atom	x	y	z
Au(1)	0.238 31(3)	0.366 88(2)	0.866 36(2)	C(3F)	−0.042 2(11)	0.429 7(5)	1.075 1(7)
Au(2)	0.248 93(3)	0.249 17(2)	0.864 35(2)	C(4F)	0.033 7(12)	0.468 3(5)	1.085 3(6)
Au(3)	0.255 57(4)	0.134 34(2)	0.895 18(3)	C(5F)	0.121 3(10)	0.473 1(5)	1.047 7(7)
P(1)	0.414 7(2)	0.361 4(1)	0.837 1(2)	C(6F)	0.132 1(10)	0.438 5(5)	0.994 8(6)
P(2)	0.432 1(2)	0.244 1(1)	0.859 8(2)	C(1G)	−0.037 3(8)	0.387 5(4)	0.849 0(5)
P(3)	0.438 5(2)	0.135 6(1)	0.919 4(2)	C(2G)	−0.017 1(9)	0.400 7(5)	0.785 5(6)
P(4)	0.067 1(2)	0.363 1(1)	0.905 7(2)	C(3G)	−0.096 3(12)	0.416 6(6)	0.740 2(7)
P(5)	0.064 7(2)	0.249 1(1)	0.866 4(1)	C(4G)	−0.199 0(11)	0.420 9(5)	0.760 5(7)
P(6)	0.074 8(2)	0.130 4(1)	0.864 0(2)	C(5G)	−0.222 3(10)	0.408 7(5)	0.822 5(7)
C(1A)	0.493 1(9)	0.419 3(4)	0.861 0(6)	C(6G)	−0.142 0(9)	0.391 8(4)	0.868 3(6)
C(2A)	0.533 4(11)	0.425 3(5)	0.923 6(7)	C(1H)	0.000 9(9)	0.265 2(4)	0.787 5(5)
C(3A)	0.585 6(11)	0.470 7(5)	0.944 2(7)	C(2H)	−0.109 2(10)	0.273 5(5)	0.779 3(6)
C(4A)	0.595 8(11)	0.509 4(5)	0.898 5(8)	C(3H)	−0.152 5(10)	0.287 3(5)	0.718 5(7)
C(5A)	0.556 5(11)	0.504 5(5)	0.834 3(9)	C(4H)	−0.091 9(13)	0.292 6(5)	0.664 9(7)
C(6A)	0.503 0(10)	0.459 1(4)	0.815 0(7)	C(5H)	0.016 9(12)	0.284 2(5)	0.671 3(6)
C(1B)	0.429 2(9)	0.351 2(4)	0.749 3(5)	C(6H)	0.062 5(10)	0.270 9(4)	0.733 1(6)
C(2B)	0.529 9(10)	0.346 9(4)	0.723 4(6)	C(1I)	0.053 8(8)	0.132 2(4)	0.776 0(6)
C(3B)	0.541 1(12)	0.336 0(5)	0.657 3(7)	C(2I)	−0.048 4(9)	0.142 3(4)	0.745 7(6)
C(4B)	0.450 9(14)	0.329 0(5)	0.617 3(7)	C(3I)	−0.059 9(11)	0.147 1(4)	0.677 7(6)
C(5B)	0.349 0(13)	0.333 9(6)	0.640 1(7)	C(4I)	0.023 3(13)	0.141 9(6)	0.637 5(7)
C(6B)	0.339 0(10)	0.345 6(5)	0.707 5(6)	C(5I)	0.122 4(11)	0.130 8(6)	0.666 5(7)
C(1C)	0.481 7(9)	0.222 2(4)	0.782 9(6)	C(6I)	0.137 9(10)	0.125 8(5)	0.735 4(6)
C(2C)	0.593 0(9)	0.215 0(4)	0.774 7(6)	C(1J)	−0.000 9(9)	0.075 5(4)	0.892 9(6)
C(3C)	0.628 6(10)	0.198 5(5)	0.715 1(7)	C(2J)	0.027 3(12)	0.026 7(5)	0.870 5(7)
C(4C)	0.557 5(13)	0.188 3(5)	0.662 2(7)	C(3J)	−0.028 9(13)	−0.017 6(5)	0.890 8(8)
C(5C)	0.449 4(11)	0.195 2(5)	0.669 9(6)	C(4J)	−0.109 0(11)	−0.012 4(5)	0.932 6(7)
C(6C)	0.411 6(9)	0.211 4(4)	0.728 5(6)	C(5J)	−0.135 4(11)	0.035 1(6)	0.955 2(8)
C(1D)	0.480 3(9)	0.103 6(4)	0.995 8(6)	C(6J)	−0.082 1(10)	0.078 7(5)	0.935 4(7)
C(2D)	0.579 0(11)	0.112 5(5)	1.027 3(6)	C(1)	0.491 6(9)	0.308 8(4)	0.877 9(6)
C(3D)	0.614 6(11)	0.081 5(5)	1.080 3(7)	C(2)	0.489 9(8)	0.203 0(4)	0.926 0(5)
C(4D)	0.552 2(12)	0.042 3(5)	1.101 9(6)	C(3)	0.022 5(8)	0.296 8(4)	0.926 5(6)
C(5D)	0.451 3(12)	0.033 1(5)	1.071 9(6)	C(4)	0.007 2(8)	0.187 8(4)	0.895 8(5)
C(6D)	0.417 1(10)	0.064 6(5)	1.018 7(6)	C(5)	0.243 1(9)	0.479 0(6)	0.763 4(6)
C(1E)	0.514 1(9)	0.103 8(4)	0.857 6(5)	C(6)	0.249 0(10)	0.252 8(7)	0.468 2(8)
C(2E)	0.628 4(10)	0.102 6(4)	0.861 1(6)	C(7)	0.229 1(10)	0.223 3(6)	0.020 1(5)
C(3E)	0.683 2(10)	0.077 6(5)	0.813 3(7)	S(1)	0.223 2(3)	0.480 3(2)	0.842 4(2)
C(4E)	0.630 5(11)	0.054 2(5)	0.760 5(7)	S(2)	0.221 2(5)	0.202 5(2)	0.511 9(3)
C(5E)	0.520 4(12)	0.053 7(5)	0.757 2(6)	S(3)	0.291 2(6)	0.286 6(3)	0.017 9(3)
C(6E)	0.462 9(9)	0.079 0(4)	0.804 1(6)	N(1)	0.258 8(10)	0.482 7(6)	0.710 2(7)
C(1F)	0.056 8(9)	0.399 7(4)	0.981 9(6)	N(2)	0.265 1(10)	0.285 4(6)	0.437 9(8)
C(2F)	−0.028 9(11)	0.395 8(4)	1.022 1(6)	N(3)	0.203 8(11)	0.194 2(7)	0.023 2(6)

Crystal data M = 2010.61, triclinic, space group $P\bar{1}$ (no. 2), a = 13.799(2), b = 14.061(2), c = 19.390(4) Å, α = 88.46(2), β = 75.41(1), γ = 74.58(1)°, U = 3506.4(1) Å^3, D_c = 1.90 g cm^{-3}, Z = 2, μ(Mo-Kα) = 86.16 cm^{-1}, $F(000)$ = 1904, dimensions 0.14 × 0.36 × 0.34 mm.

Intensities (h, $\pm k$, $\pm l$; 12 925 unique data) were measured at 22 °C on a Nicolet R3m four-circle diffractometer (graphite-monochromatized Mo-Kα radiation, λ = 0.710 73 Å) using the ω–2θ variable-scan (3.30–15.60° min^{-1}) technique at the Chinese University of Hong Kong. Azimuthal scans of selected strong reflections over a range of 2θ values were used to define a pseudo-ellipsoid for the application of absorption corrections (μr = 0.14, transmission factors 0.244–0.989).

Atomic coordinates for the Au atoms were deduced from a sharpened Patterson function, and the other non-hydrogen atoms were located from subsequent Fourier difference maps. All non-hydrogen atoms were refined anisotropically. All computations were performed on a Data General Nova 3/12 minicomputer with the SHELXTL programs.[8] Convergence for 7008 obtained data ($|F_o| \geqslant 6\sigma|F_o|$) and 691 variables was reached at R = 0.064, R_G = 0.076 and S = 2.20 with a weighting scheme w = $[\sigma^2(F_o) + 0.0004|F_o|^2]^{-1}$. The final Fourier difference map showed residual extrema in the range 0.71 to −0.62 e Å^{-3}.

Tables 1 and 2 list the atomic coordinates of non-hydrogen atoms in each complex. Selected bond distances and angles are given in Table 3.

Additional material available from the Cambridge Crystallographic Data Centre comprises H-atom coordinates, thermal parameters and remaining bond lengths and angles.

Results and Discussion

The ligand dpmp was first employed by Balch and co-workers[5,9] for the synthesis of polynuclear d^8 metal complexes. Recently, we have reported the formation of trinuclear d^{10} metal complexes **2** and **3** which display photoluminescent properties with this ligand.[1c,e] Reduction of [AuCl$_4$]$^-$ by 2,2'-thiodiethanol in methanol generated Au^I *in situ*, which rapidly reacted with dpmp. When the reaction was monitored by UV–VIS absorption spectroscopy a species having λ_{max} at ≈350 nm was formed in the early stages. Attempts to obtain it in pure form were unsuccessful as it is always contaminated with some [Au$_3$(dpmp)$_2$][SCN]$_3$. In one instance we were able to obtain crystals of this species, and the structure has been determined to be [Au$_4$(dpmp)$_2$(SCN)$_2$][SCN]Cl. The [Au$_4$-(dpmp)$_2$(SCN)$_2$]$^{2+}$ ion is unstable in solution and is easily converted into [Au$_3$(dpmp)$_2$]$^{3+}$ which is isolated as a SCN$^-$ salt. The IR spectrum of [Au$_3$(dpmp)$_2$][SCN]$_3$ displays ν(SC≡N) at 2051 cm^{-1} which is characteristic of a non-coordinating SCN$^-$ anion. The ν(SC≡N) frequency of metal-bound thiocyanate occurs at 2170–2135 cm^{-1}. The ^{31}P NMR spectrum (acetonitrile, relative to H$_3$PO$_4$) shows only two

Table 2 Atomic coordinates ($\times 10^5$ for Au, $\times 10^4$ for others) for non-hydrogen atoms of [Au$_4$(dpmp)$_2$(SCN)$_2$][SCN]Cl

Atom	x	y	z	Atom	x	y	z
Au(1)	28 602(8)	−6 299(7)	21 142(6)	C(33)	−3 701	7 544	4 757
Au(2)	12 570(6)	14 629(6)	24 828(5)	C(34)	−2 904	7 374	5 104
Au(3)	2 705(6)	36 732(6)	24 169(5)	C(35)	−1 979	6 646	4 835
Au(4)	−10 930(7)	57 705(7)	22 150(6)	C(36)	−1 853	6 088	4 218
P(1)	3 756(5)	−300(4)	2 858(4)	C(37)	−3 618(10)	5 819(12)	2 732(9)
P(2)	2 819(4)	1 788(4)	2 465(3)	C(38)	−4 515	5 564	3 100
P(3)	1 844(4)	3 994(4)	2 367(3)	C(39)	−5 397	5 809	2 835
P(4)	−2 452(4)	5 522(4)	3 051(3)	C(40)	−5 382	6 308	2 203
P(5)	−1 352(4)	3 398(4)	2 607(3)	C(41)	−4 485	6 563	1 835
P(6)	−318(4)	1 191(4)	2 463(3)	C(42)	−3 603	6 318	2 099
C(1)	3 558(15)	−848(15)	3 702(10)	C(43)	−1 923(10)	3 551(10)	1 844(7)
C(2)	3 604	−397	4 320	C(44)	−2 919	3 432	1 936
C(3)	3 479	−881	4 961	C(45)	−3 383	3 565	1 366
C(4)	3 309	−1 817	4 983	C(46)	−2 851	3 816	705
C(5)	3 263	−2 269	4 364	C(47)	−1 856	3 935	613
C(6)	3 388	−1 784	3 724	C(48)	−1 391	3 802	1 183
C(7)	5 155(9)	−676(11)	2 451(11)	C(49)	−471(14)	1 127(11)	1 565(9)
C(8)	5 824	−754	2 895	C(50)	−1 359	954	1 433
C(9)	6 897	−1 058	2 609	C(51)	−1 479	979	739
C(10)	7 301	−1 283	1 879	C(52)	−711	1 176	177
C(11)	6 632	−1 205	1 435	C(53)	178	1 348	309
C(12)	5 559	−901	1 722	C(54)	297	1 324	1 003
C(13)	3 785(12)	1 564(11)	1 596(9)	C(55)	−554(13)	98(12)	2 854(12)
C(14)	4 780	1 678	1 522	C(56)	−829	98	3 597
C(15)	5 480	1 555	851	C(57)	−995	−751	3 940
C(16)	5 186	1 319	254	C(58)	−886	−1 600	3 540
C(17)	4 191	1 206	327	C(59)	−611	−1 599	2 796
C(18)	3 491	1 329	998	C(60)	−445	−750	2 453
C(19)	2 637(10)	4 067(10)	1 478(7)	C(61)	3 446(18)	1 041(14)	3 098(13)
C(20)	3 600	4 263	1 383	C(62)	2 625(14)	3 026(13)	2 839(11)
C(21)	4 232	4 265	697	C(63)	−2 275(16)	4 220(14)	3 347(11)
C(22)	3 900	4 071	106	C(64)	−1 405(15)	2 173(13)	2 931(11)
C(23)	2 937	3 874	201	C(65)	2 811(28)	−2 175(23)	1 042(18)
C(24)	2 305	3 872	887	C(66)	−660(27)	6 460(27)	665(22)
C(25)	1 694(11)	5 158(10)	2 833(10)	C(67)	177(34)	2 650(23)	4 088(20)
C(26)	1 358	5 153	3 574	S(1)	2 092(6)	−1 051(6)	1 279(5)
C(27)	1 210	5 999	3 989	S(2)	150(5)	6 205(6)	1 317(5)
C(28)	1 398	6 852	3 663	S(3)	802(9)	1 625(9)	4 108(6)
C(29)	1 734	6 857	2 921	N(1)	3 303(27)	−2 964(19)	865(16)
C(30)	1 882	6 010	2 507	N(2)	−1 152(40)	6 873(54)	336(30)
C(31)	−2 650(13)	6 258(11)	3 871(8)	N(3)	−248(24)	3 429(24)	4 119(13)
C(32)	−3 575	6 986	4 141	Cl	5 897(9)	1 648(8)	3 246(7)

types of phosphorus nuclei in a ratio 2:1 [δ 35.04 (2P) and 30.36 (1P)]. The signal at δ 35.04 is assigned to atoms P(1) and P(3) whereas that at δ 30.36 is due to P(2) (see Fig. 1 for atom numbering). Since the chemical shifts of atoms P(1) and P(3) and that of the P atoms in [Au$_2$(dppm)$_2$]$^{2+}$ [dppm = bis(diphenylphosphino)methane][1a] are virtually identical, the NMR data are consistent with the X-ray results in that the SCN⁻ ion does not bind to the Au atoms. In solution, the major species present is [Au$_3$(dpmp)$_2$]$^{3+}$.

Crystal Structure of [Au$_3$(dpmp)$_2$]$^{3+}$.—Fig. 1 shows a perspective view of the complex cation. The cation consists of three d^{10} P$_2$Au^I units held together by the two bridging dpmp ligands. The three SCN⁻ ions can be considered as unco-ordinated as the Au $\cdots$ SCN distances range from 2.947(4) to 3.717(7) Å. The most interesting structural feature is that the Au$_3$ chain is in a nearly linear array in contrast to most trinuclear gold(I) complexes where a bent Au$_3$ chain is observed. The Au–Au–Au angle, 167.21(2)°, is closer to the ideal value of 180° than that of 136.26(4)° found in [Au$_3$(dmmp)$_2$]$^{3+}$ **4** [dmmp = bis(dimethylphosphinomethyl)methylphosphine][1b] and 110.9(1)° in [Au$_3$Cl$_3$(μ-dpma)] [dpma = bis(diphenylphosphinomethyl)phenylarsine].[10] It is also larger than the Rh–Rh–Rh angle in **1** [160.2(1)°],[5] although smaller than the Ag–Ag–Ag angle of 175.33(7)° in **2**.[1c] This structure can

thus serve as a model for a linear trinuclear gold(I) complex. The P$_2$Au units are linear with P–Au–P bond angles being 172.2(1), 176.1(1) and 176.5(1)°. Similar P–Au–P angles have been found in **4** [175.7(2)°][1b] and in [Au$_2$(dppm)$_2$]$^{2+}$ [175.2(2)°].[11] The intramolecular Au–Au distances of 3.013 7(8) and 3.004 9(8) Å are comparable to those in [Au$_2$(dmpm)$_2$]$^{2+}$ [3.028(2) Å] [dmpm = bis(dimethylphosphino)methane],[12] **4** [2.981(1) and 2.962(1) Å][1b] and [Au$_2$(dppm)$_2$]$^{2+}$ [2.982(2) Å],[11] but shorter than those of 3.201(1)–3.420(1) Å in [Au$_3$\{HC(PPh$_2$)$_3$\}X$_3$].[13] According to Schmidbaur and co-workers[13] such short intermetallic Au $\cdots$ Au contacts suggest the operation of weak metal–metal interactions. The Au–Au interaction is certainly attractive and spectroscopically significant. The Au–P distances ranging from 2.295(3) to 2.315(3) Å are normal.

Crystal Structure of [Au$_4$(dpmp)$_2$(SCN)$_2$]$^{2+}$.—Fig. 2 shows the perspective view of the complex cation with atom numbering. The structure features one of the few examples of a nearly linear tetranuclear metal complex. It consists of four two-co-ordinated Au atoms which are bridged by two dpmp ligands. The measured Au–Au–Au angles of 160.0(1) and 167.2(1)° are similar to that of 167.21(2)° for [Au$_3$(dpmp)$_2$]$^{3+}$ described above. They are, however, slightly smaller than the Rh–Rh–Rh angle of 168.0(1)° in the isostructural [Rh$_4$(μ-CO)(CO)$_2$(μ-
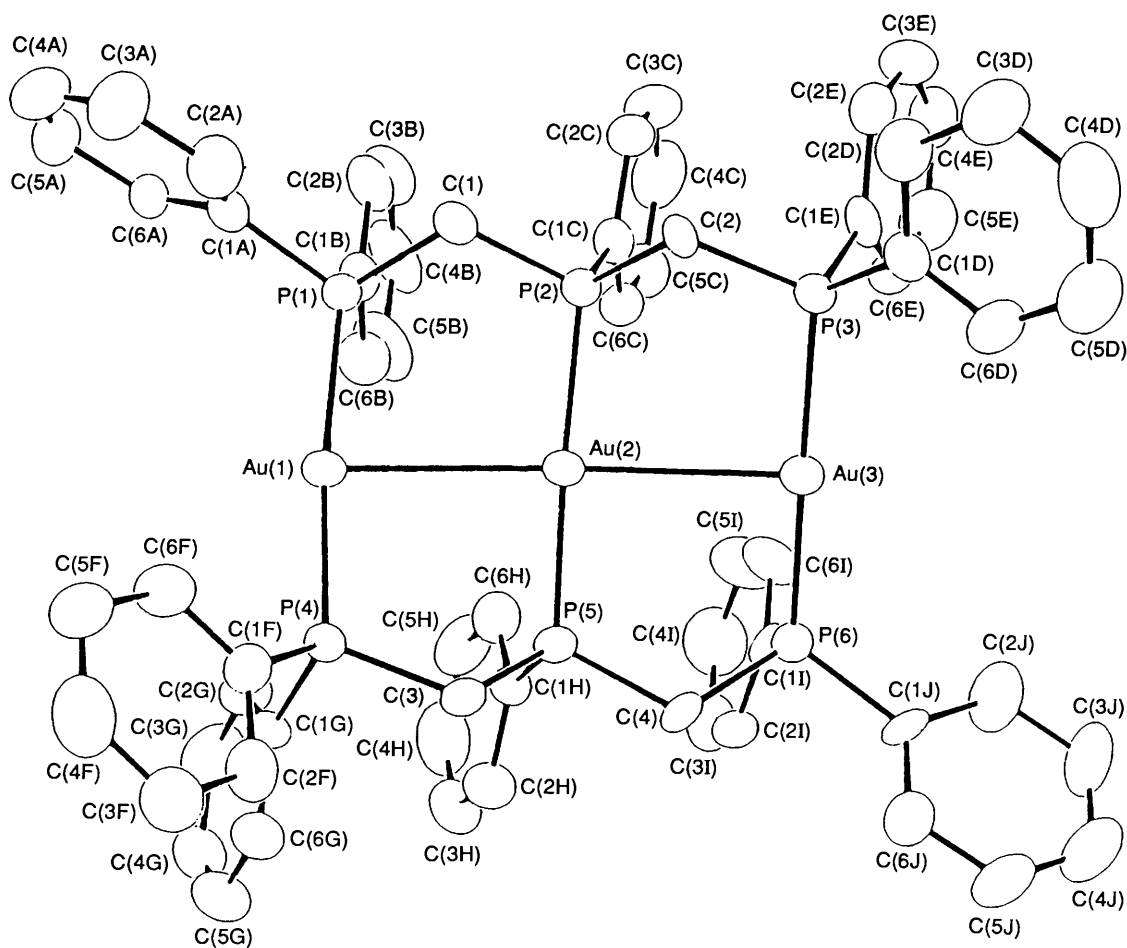
Fig. 1 An ORTEP plot of $[Au_3(dpmp)_3]^{3+}$ with atom numbering

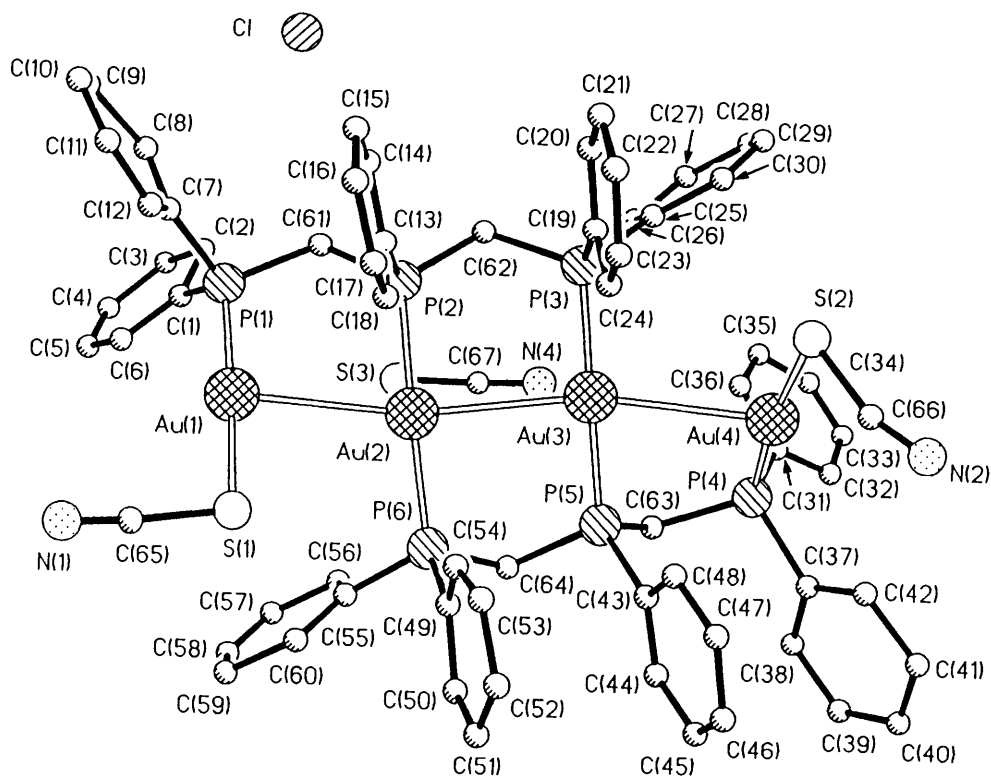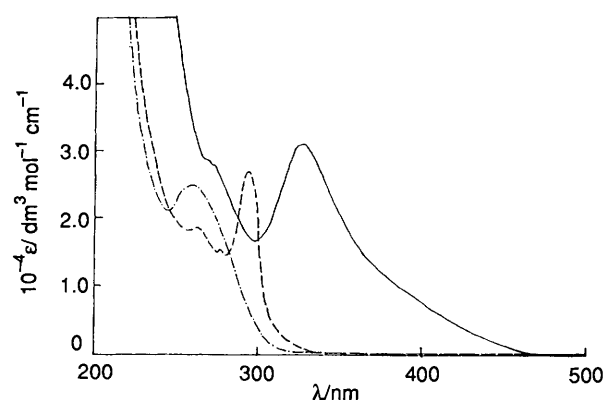**Fig. 2** An ORTEP plot of $[Au_4(dpmp)_2(SCN)_2][SCN]Cl$ with atom numbering

Table 3 Selected bond distances (Å) and angles (°)

[Au₃(dpmp)₃]³⁺	
Au(1)–Au(2)	3.013 7(8)
Au(1)–P(1)	2.308(3)
Au(2)–P(2)	2.295(3)
Au(3)–P(3)	2.312(3)
Au(2)–Au(3)	3.004 9(8)
Au(1)–P(4)	2.314(3)
Au(2)–P(5)	2.312(3)
Au(3)–P(6)	2.315(3)
Au(1)–Au(2)–Au(3)	167.21(2)
Au(2)–Au(1)–P(1)	83.87(7)
Au(2)–Au(1)–P(4)	90.28(7)
Au(2)–Au(3)–P(3)	92.68(7)
Au(2)–Au(3)–P(6)	88.13(7)
P(1)–Au(1)–P(4)	172.2(1)
P(2)–Au(2)–P(5)	176.5(1)
P(3)–Au(3)–P(6)	176.10(11)
Au(3)–Au(2)–P(2)	86.28(7)
Au(3)–Au(2)–P(5)	90.76(8)

[Au₄(dpmp)₂(SCN)₂]²⁺	
Au(1)–Au(2)	3.150(1)
Au(1)–S(1)	2.31(1)
Au(2)–P(2)	2.311(6)
Au(3)–Au(4)	3.122(1)
Au(3)–P(5)	2.310(6)
Au(4)–S(2)	2.312(8)
Au(1)–P(1)	2.250(8)
Au(2)–Au(3)	3.057(1)
Au(2)–P(6)	2.314(7)
Au(3)–P(3)	2.311(6)
Au(4)–P(4)	2.248(6)
Au(2)–Au(1)–P(1)	90.8(1)
Au(1)–Au(1)–S(1)	174.5(2)
Au(1)–Au(2)–P(2)	77.2(1)
Au(1)–Au(2)–P(6)	104.3(1)
Au(2)–Au(2)–P(6)	177.4(2)
Au(2)–Au(3)–P(3)	90.4(1)
Au(2)–Au(3)–P(5)	90.5(1)
P(3)–Au(3)–P(5)	173.3(2)
Au(3)–Au(4)–S(2)	96.4(2)
Au(2)–Au(1)–S(1)	93.6(2)
Au(1)–Au(2)–Au(3)	160.0(1)
Au(3)–Au(2)–P(2)	89.6(1)
Au(3)–Au(2)–P(6)	88.4(1)
Au(2)–Au(3)–Au(4)	167.2(1)
Au(4)–Au(3)–P(3)	101.4(1)
Au(4)–Au(3)–P(5)	78.4(1)
Au(3)–Au(4)–P(4)	91.0(1)
P(4)–Au(4)–S(2)	172.4(2)

Cl)₂Cl₂(dppy)₂][dppy = 2,6-bis(diphenylphosphino)pyridine].[14] In the related [Au₄Cl₂(μ-dpma)₂]²⁺ system[5] the Au₄ chain is bent with a Au–Au–Au angle of 88.0(1)°. The bent Au₄ chain has previously been attributed to Au–Au bonding interaction. Perhaps the nearly linear Au₃ and Au₄ chains found in this work are due to the constraining effect of the dpmp ligand, which becomes an important factor in affecting the structure. It should also be remembered that the Auᴵ–Auᴵ interaction is weak. The measured Au(2)–Au(3) distance of 3.057(1) Å is similar to that for [Au₃(dpmp)₂]³⁺ as discussed above. The Au(1)–Au(2) and Au(3)–Au(4) distances of 3.150(1) and 3.122(1) Å are slightly larger, perhaps due to the co-ordination of SCN⁻ to atoms Au(1) and Au(4). Because Auᴵ is considered to be soft, it is not unreasonable to find that the SCN⁻ ligand is S-bonded to the Au atoms. The Au–P and Au–S distances are normal.

Spectroscopic and Photophysical Properties.—Fig. 3 shows the room-temperature UV–VIS absorption spectra of [Au-

Fig. 3 The UV–VIS absorption spectra of [Au(PPh₃)₂][CF₃SO₃] (– · – · – ·), [Au₂(dppm)₂][CF₃SO₃]₂ (– – – –) and [Au₃(dpmp)₂]-[SCN]₃ (———) in acetonitrile at room temperature

(PPh₃)₂][CF₃SO₃], [Au₂(dppm)₂][CF₃SO₃]₂ and [Au₃-(dpmp)₂][SCN]₃ in acetonitrile. The corresponding spectrum of a crystal of [Au₄(dpmp)₂(SCN)₂][SCN]Cl recorded in one instance showed a broad absorption band at ≈ 350 nm. The spectra are dominated by the intense absorption at $\lambda_{max} = 259$ nm ($\varepsilon_{max} = 2.5 \times 10^4$) for [Au(PPh₃)₂]⁺, 295 ($\varepsilon_{max} = 2.72 \times 10^4$) for [Au₂(dppm)₂]²⁺, 326 ($\varepsilon_{max} = 3.16 \times 10^4$ dm³ mol⁻¹ cm⁻¹) for [Au₃(dpmp)₂]³⁺, 350 nm for [Au₄(dpmp)₂(SCN)₂]²⁺.

The molecular orbital diagram for bi- and tri-nuclear gold(I) phosphine systems has been discussed before.[1b] One would expect [Au₄(dpmp)₂(SCN)₂]²⁺ to have a similar diagram although the energy gap between the p_σ and d_δ* (or d_σ*) orbitals is reduced. Here, the p_σ(p_σ*), d_σ(d_σ*) and d_δ(d_δ*) orbitals come from the symmetric (antisymmetric) combination of the 6p_z, 5d_z² and (d_xy, d_x²–y²) orbitals respectively. The Au–Au–Au axis is defined to be the Z axis. It is likely that configurational mixing between the p_σ and π* (dpmp) orbitals may exist. For symmetry reasons, the d_δ* ——→ p_σ transition is expected to be less intense than that of d_σ* ——→ p_σ. The electronic absorption spectrum of [Au₃(dpmp)₂]³⁺ shows an intense band at 326 nm and a weaker one (shoulder) at around 350 nm. By analogy to the well established pattern in d⁸–d⁸ species[5,15] and previous work on the related d¹⁰–d¹⁰ system,[1b] the intense band of [Au₃(dpmp)₂]³⁺ at 326 nm is attributed to the spin-allowed d_σ* ——→ p_σ transition and the weaker one to the d_δ* ——→ p_σ transition. The stacking of P₂Au units results in an attractive Au–Au interaction. As the number of P₂Au units increases the d_σ*–p_σ energy gap narrows and the energy of the d_σ* orbital increases. Thus it is not unreasonable to find that [Au₄(dpmp)₂(SCN)₂]²⁺ absorbs at a lower energy than does [Au₃(dpmp)₂]³⁺. A similar red shift in the d_σ* ——→ p_σ transition has been reported in polynuclear d⁸ systems.[1b]

The complex [Au₄(dpmp)₂(SCN)₂][SCN]Cl has been found to display an intense yellow emission upon UV–VIS excitation; however, its photophysical properties have not been investigated in detail because of the lack of a reliable synthesis of this complex. Upon excitation at 300–400 nm a degassed acetonitrile solution of [Au₃(dpmp)₂][SCN]₃ displays intense photoluminescence at room temperature. As shown in Fig. 4, there are two emissions centred at 600 and 500 nm, the latter one appearing as a shoulder. The emission lifetimes have been measured to be 1.0 and 3.7 μs for the high- and low-energy emissions respectively. Since the free dpmp ligand exhibits broad and weak emission from 420 to 500 nm in acetonitrile at room temperature, the emission at 500 nm likely comes from intraligand spin-forbidden transitions. The lowest-energy emitting electronic state is unlikely to be derived from the ³[(d_σ*)¹(p_σ)¹] state because of the relatively small difference in emission energies between [Au₂(dppm)₂]²⁺ (emission band centred at 570 nm)[1a] and the present system, and the very large
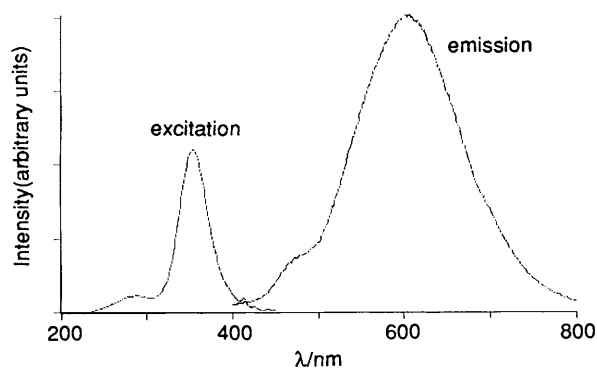
Fig. 4 Emission and excitation spectra of $[Au_3(dpmp)_2][SCN]_3$ in degassed acetonitrile at room temperature

Stokes shift observed between the $d_{\sigma^*} \longrightarrow p_\sigma$ transition energy and the emission at 600 nm. We suggest that the latter emission of $[Au_3(dpmp)_2]^{3+}$ comes from the low-lying $^3[(d_{\sigma^*})^1(p_\sigma)^1]$ state. Its quantum yield was measured to be 1.4×10^{-3} (excited at 400 nm). Similar emission (maximized at 610 nm) could also be observed in a solid-state sample at room temperature. Cooling the sample to 77 K only leads to an increase in emission intensity. No vibrational fine structure has been observed.

Acknowledgements

References

1 (a) C. M. Che, H. L. Kwong, C. K. Poon and V. W. W. Yam, J. Chem. Soc., Dalton Trans., 1990, 3215; (b) V. W. W. Yam, T. F. Lai and C. M. Che, J. Chem. Soc. Dalton Trans., 1990, 3747; (c) C. M. Che, H. K. Yip, S. M. Peng, G. H. Lee, Y. M. Wang and S. T. Liu, J. Chem. Soc., Chem. Commun., 1991, 1615; (d) C. M. Che, H. K. Yip, V. W. W. Yam, P. Y. Cheung, T. F. Lai, S.-J. Shieh and S. M. Peng, J. Chem. Soc., Dalton Trans., 1992, 427; (e) D. Li, H. K. Yip, C. M. Che, Z. Y. Zhou, T. C. W. Mak and S. T. Liu, J. Chem. Soc., Dalton Trans., 1992, 2445.
2 C. King, J. C. Wang, N. I. Md. Khan and J. P. Fackler, jun., Inorg. Chem., 1989, 28, 2145; N. I. Md. Khan, C. King, D. D. Heinrich, J. P. Fackler, jun. and L. C. Porter, Inorg. Chem., 1989, 28, 2150.
3 C. M. Che, W. T. Wong, T. F. Lai and H. L. Kwong, J. Chem. Soc., Chem. Commun., 1989, 243.
4 D. Perreault, M. Drouin, A. Michel and P. D. Harvey, Inorg. Chem., 1991, 30, 2.
5 A. L. Balch, L. A. Fossett, J. K. Nagle and M. M. Olmstead, J. Am. Chem. Soc., 1988, 110, 6732.
6 R. Appel, K. Geisler and H. F. Schöler, Chem. Ber., 1979, 112, 648.
7 C. A. McAuliffe, R. V. Parish and P. D. Randall, J. Chem. Soc., Dalton Trans., 1979, 1730.
8 G. M. Sheldrick, in Computational Crystallography, ed. D. Sayre, Oxford University Press, New York. 1982, p. 506.
9 R. R. Guimerans, M. M. Olmstead and A. L. Balch, J. Am. Chem. Soc., 1983, 105, 1677.
10 A. L. Balch, E. Y. Fung and M. M. Olmstead, J. Am. Chem. Soc., 1990, 112, 5181.
11 L. C. Porter, N. I. Md. Khan, C. King and J. P. Fackler, jun., Acta Crystallogr., Sect. C, 1989, 45, 947.
12 H. H. Karsch and U. Schubert, Z. Naturforsch., Teil B, 1982, 37, 186.
13 A. Stützer, P. Bissinger and H. Schmidbaur, Chem. Ber., 1992, 125, 367.
14 F. E. Wood, M. M. Olmstead and A. L. Balch, J. Am. Chem. Soc., 1983, 105, 6332.
15 D. M. Roundhill, H. B. Gray and C. M. Che, Acc. Chem. Res., 1989, 22, 55.